ABSTRACT

Wall conditioning will be required in ITER to control fuel and impurity recycling, as well as tritium (T) inventory. Analysis of conditioning cycle on the JET, with its ITER-Like Wall is presented, evidencing reduced need for wall cleaning in ITER compared to JET-CFC. Using a novel 2D multifluid model, GDC current density on the in-vessel plasma-facing components (PFC) of ITER is predicted to approach the simple expectation of total anode current divided by wall surface area. Baking of the divertor to 350°C should desorb the majority of the co-deposited T. ITER foresees the use of low temperature plasma based techniques compatible with the permanent toroidal magnetic field, such as Ion (ICWC) or Electron Cyclotron Wall Conditioning (ECWC), for tritium removal between ITER plasma pulses. Extrapolation of found ICWC efficiencies to ITER indicates removal comparable to estimated T-retention in nominal ITER D:T shots, whereas GDC may be unattractive for that purpose.

1. INTRODUCTION

Wall conditioning of tokamaks is a common tool to influence fuel – and impurity recycling and to improve plasma performance and reproducibility [1]. In common with present tokamaks, it will be required in ITER to control the surface state of plasma facing components, easing plasma initiation, fuel or impurity recycling and isotopic ratio control. It will occur either before plasma operation after torus vacuum vessel openings, or during operation. Wall conditioning will be used to remove of medium and medium-high Z impurities from the ITER Beryllium (Be) first wall and Tungsten (W) divertor surfaces, in order to keep uncontrolled impurity radiation caused by their release from plasma facing components as low as possible and thereby maximize plasma performance or prevent disruptions. Wall conditioning will also be used to deplete hydrogenic layers formed from wall surfaces in order to control release of hydrogenic atoms/molecules, and thus plasma density in order to ensure reliable discharge initiation. It will be needed after the use of extrinsic impurities, or after disruptions, both potentially leading to the absorption or implantation of medium-high Z impurity on wall surfaces. In the nuclear phase of ITER, wall conditioning will certainly contribute to the control of the tritium (T) inventory within the fuelling cycle – a major safety issue since the agreed sfety limit inside the vessel must be kept under 640gT during D:T operation [2] – by depleting Tritium from the walls and in particular from that co-deposited with Beryllium.

ITER is currently envisioning several techniques for the conditioning of the vacuum vessel. Hence, conventional techniques like baking and glow discharge cleaning (GDC) will be used on ITER for both impurity of T removal. In ITER however, the magnetic field, generated by superconducting coils, will be continuously maintained. Conventional DC-glow discharges being unstable in the presence of such an intense magnetic field, methods compatible with the permanent toroidal magnetic field of ITER, such as Ion (ICWC) [3, 4] or Electron Cyclotron Wall Conditioning (ECWC) [5], are foreseen in ITER for fuel and impurity removal between plasma pulses.

This paper reviews the current experimental and modeling activities on the currently envisioned

techniques for the conditioning of ITER vacuum vessel. A first part is devoted to baking and GDC for impurity and T removal in ITER. In a second part, current R&D activities on ICWC and ECWC are reviewed, and the efficiency of these techniques is discussed, in particular for their application to control of the T inventory in ITER. Results and conclusion for ITER are summarized in a third part.

1. BAKING AND GDC

A. REDUCED NEED FOR WALL CLEANING ON JET-ILW

Baking of the ITER vacuum chamber, particularly in conjunction with Glow Discharge Conditioning, is the one of the primary conditioning techniques which ITER will use to prepare in-vessel component surfaces prior to machine start-up and thereafter for plasma operations following maintenance procedures requiring in-vessel access. Baking, GDC and their impact on operation have been in particular studied in JET ITER-Like-Wall (ILW) [6], its wall material mix [7] providing results of particular relevance to ITER.

Since the PFC change in 2011, JET-ILW has been vented three times for tile exchange or maintenance. Four conditioning cycles have been performed, the first one (i) – baking at 200°C and 320°C and about 215 hours D2-GDC (among which 65 hours at 200°C) – having been performed on pristine PFCs [6]. The three other cycles operated on JET-ILW consisted in (ii) baking at 200°C and 100h GDC, (iii) baking at 200°C and 100 GDC (among which 6 hours GDC in air accidentally operated) and (iv) baking at 320°C and 50 hours GDC, followed by 50 hours GDC at 200°C. During the first cycle, intermittent D_2 glow discharges ($p = 3.10^{-3}$mbar, I = 15A, U = 500Volts) with a total duration of 150 hours at 320°C and 65 hours at 200°C, allowing reaching a 2MA target current after only 5 shots, whereas it took about 45 shots in 2008 on JET-CFC [6].

The use of Be as PFC material in the ILW has proven to have a large impact on the conditioning cycle, the most noticeable being the absence of any further need for wall conditioning after the initial plasma restart, dramatically contrasting with restart and operation in JET with CFC-dominated walls [6]. As in ASDEX-Upgrade, the control of tungsten sources appears to be also essential in the JET-ILW to avoid too high radiation levels in the plasma core and degradation of confinement and performances [8]. Recent experiments comparing identical H-mode plasmas before or after Be evaporation suggest strong W sources in the main chamber, dominating the plasma contamination with respect to divertor sources [9]. Be evaporation, which have been so far conducted in JET-ILW only in this aim, are however not foreseen in ITER.

The temporal evolution of the oxygen V line intensity at 629Å, measured in the plasma core either in the first 3 s following breakdown or after X point formation is shown on Figure 1 for several experimental JET-CFC and JET-ILW campaigns. Grey dashed lines on Figure 1 represent the GDCs that were needed to reduce impurity content, which frequency of operation is drastically reduced with respect to operation with carbon dominated PFCs. Carbon levels are even more reduced [10], but since ITER is not considering carbon as PFC anymore, they are not shown here. Thanks to the getter capabilities of beryllium, and despite an air leak present in the first restart with

the ILW (from JET Pulse No: 80128), the oxygen level is a factor of 10 lower in the first restart compared to previous ones with JET-CFC (from JET Pulse No: 70966). From Figure 1 it is also clear that oxygen levels slightly increase later throughout campaigns. This is particularly obvious in breakdown phases – when the plasma leans on Be limiters – of plasmas in restarts following that of the first operation of JET-ILW with pristine PFCs. O levels are plotted on Figure 2 as a function of the number of shots after the four cycles. The increase is attributed to the formation of BeO, eroded and/or re-deposited on Be surfaces, but could also be caused by the lower baking temperature and/or shorter GDC durations in some of the conditioning cycles after the first operation of JET-ILW, although no clear trend on O (or other impurities like water) removal efficiency could be so far firmly identified with respect to these. However, from an operational point of view, it clear that the increase of O contamination has a slight impact on restart (but still limited compared to previous restarts in JET-CFC), making it more difficult to reach target plasma current as in the first restart with ILW [6].

B. FUEL REMOVAL BY BAKING

The ITER First Wall and the divertor can be baked up to 240°C and to 350°C respectively and baking is one option for partial tritium recovery in the nuclear phase. Although both beryllium and tungsten present the advantage of significantly reducing hydrogenic fuel retention, compared with carbon, as demonstrated in JET-ILW [11], co-deposition of tritium with eroded plasma facing material is expected to be the main cause of retention in the nuclear phase of ITER. The estimated T-retention lies between 0,14 and 0,5gT per 400s long ITER D:T shots [11, 12] and the administrative limit of 640gT may thus be reached after a few thousands nominal shots [2], [11]. Laboratory experiments suggest that almost all tritium should desorb from co-deposited “pure” Be layers at 350°C, up to 90% of the initially co-deposited fuel being thermally released after 24 h at this temperature [13, 14]. Desorption of D implanted in Be-containing mixed materials (W, C) was found to be less efficient [15], the amount of released fuel decreasing with the amount of W or C in the layer. For D implanted in Be, the amount of fuel that can be released is reduced if the implantation temperature is increased. Hence, for implantation temperatures higher that of baking, tritium cannot be released, even from pure Be layers. It is reported in [15] that only about 50% of fuel implanted at 423K can be released at 623 K, which may limit the efficiency of baking in this case. Significantly lower fuel content in co-deposited Be layers is however expected as the temperature at which co-deposits are formed [15, 16].

Baking of the divertor cassettes will be possible in ITER up to 350°C by circulation of hot pressurized N_2 in the divertor cooling circuits. This will require drying and draining of the divertor beforehand, which may last a week. Baking frequency is not clearly established, but it is estimated that it should performed between two and 8 times a year to keep the T inventory under the 640g limit [12], or during forecasted major plasma shut down.

C. PERFORMANCE OF THE GLOW DISCHARGES SYSTEM OF ITER

The ITER GDC system consists of 7 anodes housed in the outer midplane and upper lateral port plugs, forming an integral part of the diagnostic shield modules mounted on the port plug front ends, directly facing the plasma. GDC in ITER will be run at a discharge current up to 30A per anode, in the pressure range of 0.1 – 1 Pa [17]. The performance of the proposed GDC system and in particular the expected distribution of glow plasma current density on the in-vessel plasma-facing components (PFC) has been for the first time simulated using a novel self-consistent 2D multi-species fluid model [18], benchmarked beforehand against experimental data from glow discharges produced both a small scale laboratory experiment and in JET and RFX toroidal devices, with reasonable agreement [19], [20]. Glow discharges in tokamaks behave as hollow cathode discharges [18–21]: the discharge is sustained by fast electrons emitted from the cathode by ion impact, accelerated through the cathode fall, penetrating the plasma volume as a fast electron beam and trapped in the bulk discharge by the cathode fall surrounding the plasma. In addition to hydrogen ion species (H^+, H_2^+, H_3^+) the model this describes two populations of electrons by separate sets of fluid equations: slow electrons in the bulk rapidly thermalized by inelastic collisional processes, and fast secondary electrons accelerated in the cathode sheath (several 100V) and trapped in the potential well formed by the cathode fall surrounding the plasma on all sides. These fast electrons are responsible for the creation of nearly uniform plasma all over the vessel surfaces.

Due to the relatively small anode surface area compared to the vessel area (~ 1/2000 in ITER), an additional glow forms around the anode in order to increase the local plasma density and electrical conductivity and enable current continuity. This results to higher ion current density to the vessel walls in the vicinity of the anode by up to a factor of 100, decreasing as a function of distance to the anode. Figure 3 shows the spatial distribution of plasma density, temperature and potential in a simulated H2-GDC in ITER at 0.3 Pa. The anode voltage for these conditions is 375V, the discharge current being fixed at 30A. Two concentric spheres are used to model the ITER vacuum vessel, keeping surface area and aspect ratio constant [18]. The simulations predict that ITER H2-GDC plasmas, created by one or two anodes, will be reasonably homogenous in terms of plasma density, temperature and potential, provided that the gas pressure ranges between 0.2 – 0.5Pa, which is a common pressure domain for GDC in present fusion devices. Similarly, the GDC current density onto wall surfaces, which determines the rate of cleaning, is likely to be very homogenous at reasonably short distances from the anodes (for the pressures considered here), even in case of operation with one or two anodes, and will closely approximate the simple expectation of total anode current divided by the wall surface area ($0.03 A/m^2$ per anode), the current density profile flattening as the number of anodes increases. Simulated current density distributions along the toroidal disstance from a powered anode are plotted on Figure 4, for the same total current as in Figure 3, but at different pressures. For pressures below 0.5 Pa, the ion current distribution and glow homogeneity change little, independent of the number of anodes. There is therefore probably no real benefit to operate ITER glow discharges at pressures lower than this value, given that this may lead to penalties with

respect to overheating of the water-cooled anodes if the pressure is too low. It is thus reasonable to expect a much higher degree of GDC plasma uniformity with a higher wall ion current density when all planned 7 anodes are used simultaneously (0.21 A/m2). This value is comparable to GDC ion fluxes in JET (0.10 A/m^2), RFX and TORE SUPRA (0.06 A/m^2) and ASDEX-Upgrade (0.20 A/m^2).

Simulations also predict a higher degree of glow plasma homogeneity in He compared with H, as observed on TORE SUPRA and reported in [22] for JET, and as expected from the shorter mean-free-paths for ionization and momentum transfer, and the simpler chemistry in He.

D. FUEL REMOVAL BY GDC

Fuel removal efficiency of GDC has been assessed after six months of the first deuterium campaign in the JET-ILW [6]. For this the ILW was preloaded by 30 min D_2-GDC ($p = 3.10^{-3}$ mbar, I = 15A, U = 500Volts) and gas injection was switched to H_2, keeping pressure and voltage constant. Isotopic exchange between the discharge and the wall was assessed from partial pressure measurements in the exhausted gas by means of mass spectrometry. The temporal evolution of the exhausted hydrogen (red) and deuterium (blue) fluxes during change-over from D_2 to H_2-GDC at $t \sim 0$ is plotted on Figure 7. About 3.10^{22} wall D atoms could be replaced by H atoms within the first 140s of H_2-GDC, the amount of exhausted D atoms reaching 10^{23} after nearly one and a half hour discharge time. Gas balance between injected and pumped particles did not evidence any additional wall saturation by H_2-GDC, even after this time, H retention proceeding at a similar rate than D removal [6]. From the decay of the exhausted D on Figure 7, it is expected that only little additional fuel may be removed for longer GDC durations. Roughly extrapolated to ITER, about a mole of T could be removed by D_2-GDC in a similar duration. However GDC can only be operated in the absence of the toroidal or poloidal magnetic field [23]. In ITER, the number of cycles of the superconducting toroidal field coils will be limited to 1000 for their whole lifetime [24]. This means practically that the confinement magnetic field will be continuously maintained or that the coils may be de-energized and energized at a maximum frequency of once a week. This operational constraint and the above mentioned efficiencies of GDC for fuel removal, probably render GDCs unattractive for the purpose of T inventory control in ITER.

2. ION AND ELECTRON CYCLOTRON WALL CONDITIONING

Several techniques alternative to GDC and which are compatible with B are under development or used in today's experiments, among which Taylor Discharge Cleaning or High Frequency Glow discharges. Ion Cyclotron Wall Conditioning (ICWC) and Electron Cyclotron Wall Conditioning (ECWC), techniques compatible with the intense toroidal magnetic field, are integrated into the ITER baseline as a functional requirement of the Ion Cyclotron Resonance Frequency (ICRF) and Electron Cyclotron Resonance Frequency (ECRF) heating systems respectively [25]. ITER plasma control systems are now including these wall conditioning methods [26], which require control

of a number of ITER plant systems, including the heating system itself as well as gas input and possibly poloidal field.

A. PRINCIPLE OF ICWC AND SCENARIOS IN ITER

ICWC has been the subject of considerable study on current tokamaks [3], [4], [27–32]. The principle of ICWC discharge production, in the presence of the toroidal magnetic field, has been described elsewhere (see e.g. [3], [30]). Coupling of the RF to the ICWC discharge mainly results from collisional absorption of the RF energy by the electrons (non-resonant coupling) accelerated in the parallel electric field close to the antenna. ICWC discharges present poloidal and radial non-uniformities inherent to the fact RF waves (10–100MHz) are not propagating in vacuum. Complex wave absorption schemes, including Ion Cyclotron Resonance (ICR) absorption and mode conversion [3], [30], and/or operation in monopole phasing [4], [30] are required to improve discharge homogeneity and optimize wall coverage [4]. ICWC discharges are produced at low density (between 10^{16} and $10^{18}m^{-3}$) and low temperature ($1 < T_e < 10eV$).

The main flux to the wall is that of isotropic neutral hydrogenic species either desorbed from the wall surfaces [28] or created by dissociation of molecular hydrogen by electron collisions, these having Franck-Condon energies of a few eV. In addition to ion fluxes parallel to the magnetic field lines, fast neutrals are produced in ICWC by charge exchange between protons or deuterons accelerated in the ICR layer and the background neutral gas, with temperatures above 1keV and energies up to 50keV, making them particularly attractive for T-removal [32]. These will be discussed in section 2.c below. The radial distribution of the parallel ion flux was measured in a TORE SUPRA He-ICWC plasma with a vertically reciprocating Retarding Field Analyser. It is shown in Figure 5. The red and blue points represents ion current measured at the ion and electrons side collectors of the probe respectively. Above $z > 0.8m$, where no long magnetic connections exist anymore [33] ion current decrease exponentially until zero. i.e. in the edge of the ICWC discharge. The exponential decrease is characterized by Bohm diffusion in the edge of ICWC plasmas [28, 33]. Ion wall flux is thus the largest on the first limiting surfaces, reaching here 10^{21} ions.m^{-2} on the first limiting surfaces, which is to be compared with ion flux in a GDC of typically 4 orders of magnitude below (see section 1.c).

In ITER, the use of ICWC implies that the toroidal field is either fixed at 2.65T (He:H phase) or 5.3T (D:T phase). With RF frequencies of the ICRH generators ranging from 40 to 55MHz, and thus f/B_T values of 7.5 – 10.5MHz/T, Ion Cyclotron Resonance (ICR) layers for D^+ ions at $B_T = 5.3T$ lie on ITER's magnetic axis between $\rho = 0$, i.e. above the divertor, and at $\rho = -0.6$, respectively. At $B_T = 2.65T$, ICR layers for the protons lie at the same positions at the same frequencies. Extrapolation of operational parameters from current experiments indicate that ICWC could be operated with 3–5MW RF power at input pressures ranging between 10^{-3} and 10^{-1} Pa in ITER.

B. PRINCIPLE OF ECWC AND SCENARIOS IN ITER

ECWC can also be easily produced in the presence of the toroidal magnetic field. Many experiments were however performed using microwave frequencies close to 2.45GHz at $B_T \leq 0.1$T [34]. The use of frequencies above 110GHz has been less and only recently investigated on TEXTOR, JT-60U, KSTAR and TORE SUPRA [5], [35, 36]. ECWC is foreseen as the sole conditioning method in the presence of the toroidal field in JT-60SA and W7-X. As ICWC, ECWC will be used in ITER at half or full field, using both the fundamental and first harmonic Electron Cyclotron Resonance (ECR) at $\omega = qB_T(R)/n.m_e$, n = 1 and 2 respectively, somewhat at the High Field Side, to match ITER gyrotron frequency of 170GHz. In this respect, ECWC operation is very similar to that of ECRH-assisted breakdown [37] envisioned in ITER, which is a functional requirement of the ECRH system [25], with discharges produced in the same pressure range in both cases.

As in ICWC, but in a greater extent, localized power deposition and high density in ECWC plasmas (about 10^{18}–10^{19} m^{-3}) can affect discharge uniformity and cleaning efficiency. The latter can be enhanced by pulsed operation [4], [27], which minimizes re-ionization and re-implantation of wall desorbed species, as it will be discussed below. Another drawback of the technique is the low ECR power absorption per pass in the vacuum vessel. As the beam is injected into the neutral gas, a fraction of the ECR power is absorbed by the electrons at the location of the ECR resonance, while the remaining power is reflected by the facing wall surfaces, diffused, de-polarized and damped on in-vessel components and an undefined mixture of O- and X-mode polarization will fill the whole vessel [37]. It is therefore important to ensure sufficient absorption of the ECR power in order to avoid exposure of plasma facing components or diagnostics to excessive stray radiation which may damage them. Although ECWC densities are higher than those typically encountered in ICWC discharges, they are far below cut-off densities in current devices. At fundamental ECR, power absorption in low density ECWC discharge depends little on the polarization of the wave. On the other hand, in low temperature ECWC discharge, ECR power absorption is much less efficient for first harmonic than at fundamental frequency [37]. In the latter case, the few electrons created upon ionization of the neutral gas at the intersection of EC beam and ECR surface are rapidly lost to the walls, due to the vertical drift $\nabla B \times B$, magnetic connection lengths being moreover halved at half BT. As a consequence, ECWC plasma production remains much more localized.

Localized power deposition can be compensated by the application of a weak poloidal field. Radial extension has been successfully demonstrated on JT60-U [5] and TORE SUPRA at the fundamental ECR and in KSTAR [36] for the both cases of fundamental and first harmonic absorption. The increase of wall coverage could be clearly correlated to the cleaning efficiency on TORE SUPRA. Figure 6 which shows the increase of partial pressures – and thus wall release in two He-ECWC discharges on TORE SUPRA (B_T = 3.8T, f = 110GHz, $p_{He} = 5.10^{-2}$Pa). Short pulse duration of 50ms were used followed by post-discharge time, shorther without (full lines) and with (dashed lines) application of a small radial field.

Whereas in the fundamental ECR scenario, a small radial field proved to extend discharge

uniformity and plasma wetted area significantly, a more complex poloidal field pattern is required to improve uniformity in ECWC scenarios at the first harmonic to compensate $\nabla B \times B$ drift and confine the accelerated electrons in the vicinity of ECR resonance [36]. In KSTAR, it was also found that toroidal injection angle up to 20° (minimum injection angle of ITER) did not much affect discharge production [36]. Current data suggest ECWC operation in ITER with 3–10MW (this high value is extrapolated from [5]) ECRF power at pressures between 10^{-3} and 10^{-1}Pa.

C. IMPURITY AND FUEL REMOVAL BY ICWC AND ECWC

Efficiency of ICWC and ECWC for fuel removal has been assessed on several current tokamaks. Both techniques have been for instance successfully used to recover from disruption in TORE SUPRA with ICWC, [4] and in JT-60U with ECWC [5], Encouraging results for the recovery of W wall surface state after massive gas injection (MGI) have been obtained on ASDEX-Upgrade, using six 10s long He-ICWC (f = 30MHz, B_T = 2.0T) discharges, allowing removing almost all Ar atoms implanted in the W surfaces by glow discharges beforehand [38]. Ar removal was for the first time correlated with the presence of fast CX neutrals in He-ICWC. This result, apparently in contradiction with previous finding on JET-CFC indicating on minor role of fast CX in D_2-ICWC, is now understood and explained by dominant Ion Cyclotron Resonance absorption in He-ICWC discharges, whereas collisional absorption by electrons dominates in hydrogenic ICWC discharges [38], [39].

High isotopic exchange between H_2-ICWC plasma and the TORE SUPRA walls was for the first time quantified in [4]. The observed accompanying progressive wall saturation by H_2 or D_2-ICWC, attributed to much lower residence time of wall desorbed particles compared τo characteristic pumping time in current devices, is now regularly mitigated by pulsing ICWC plasmas [4], [27].

Deuterium and hydrogen ICWC operation in equivalent ITER full or half field scenario has been in particular investigated in the largest present-day tokamak JET, allowing assessing the efficiency of the technique for fuel removal on the ITER material mix and compare with previous results in JET-CFC [4]. Experiments were performed either at ITER-relevant f/BT value in Deuterium (B_T = 3.3T and f = 25MHz, with on-axis $\omega = \omega_{CD}+$) or in Hydrogen (B_T = 1.65T and f = 25MHz, with on-axis $\omega = \omega_{CH}+$). Whereas H_2-GDC was used to preload wall surfaces in ITER full field D_2-ICWC, ITER half field H_2-ICWC has been operated at the end of the second deuterium JET-ILW campaign, without artificial preloading beforehand.

Efficiency is assessed either by monitoring the partial pressures of the masses of interest, either using absolutely calibrated quadrupole mass spectrometers (QMS) or optical penning gauges (JET), or analyzing the gas collected throughout a whole experimental session by means of gas chromatography. Table 1 gives particle balances, integrated over the cumulated RF duration of each experimental session.

In the three cases, wall retention was limited by the long silent time between each ICWC pulse, as discussed above. The isotopic ratio X/(D+H), with X = H or D the wall specie, measured during

discharges or in the exhausted gas, given on Figure 8, decreases down to a minimum value of 10–15% in ICWC discharges operated in the JET-ILW, without cryopumping [40]. The accessible reservoir for isotopic exchange, i.e. the amount of wall atoms that can be replaced by the ICWC discharge specie, ranges between $1{,}6.10^{22}$ for JET-CFC to 6.10^{22} in JET-ILW depending on the discharge cumulated duration, with an approximately equivalent wall retention. Almost twice faster isotope removal is reported on the ILW [40], in agreement with integrated removed amount in Table 1 for D_2-ICWC of similar cumulated RF durations. Despite stabilization of the isotopic ratio in the discharge at 5–10%, the cumulated amount of exhausted D atoms by pulsed H_2-ICWC (21 discharges) applied on the naturally loaded JET-ILW (without preloading beforehand) is found to be similar or higher with ICWC than that accessible by ohmic pulses [41], showing no sign of saturation after 206s cumulated RF discharge duration [40].

Efficiency of ECWC for fuel removal has been less investigated in current devices. Available data in the literature is scarce, indicating however lower fuel removal capabilities in Helium discharges than in ICWC TEXTOR-94 [35], in the WEGA stellerator [42] and in TORE SUPRA. In hydrogen however, similar efficiencies were reported on WEGA with both techniques [42]. The renewed interest by the community to this technique for the conditioning of JT-60SA and W7-X will certainly correct this lack of data.

3. SUMMARY AND CONCLUSIONS FOR ITER.

Like in all tokamaks, ITER foresees the use of baking and GDC prior restart and operation to clean wall surfaces after shut-down or maintenance. In this respect, the analysis of the conditioning cycles and the survey of impurity levels throughout the experimental campaigns of JET-ILW consolidate these options in ITER. Build-up of Be layers resulting in higher O contamination in the limiter phases of JET-ILW plasmas does not appear to impact significantly operation, compared to restarts in JET-CFC.

2D multi-fluid modeling [18-20] of glow discharges has help providing physics input to the design of the new GDC system [17], evidencing adequate toroidal and poloidal ion current density distribution, with relevant ion fluxes to the wall [19, 20].

Baking of the divertor to 350°C is the main technique for T-removal in ITER. However, it will only be performed during major ITER shut-down, the sole temperature ramp-up and ramp-down sequence requiring a week of operation. As estimated in [12], divertor baking should be operated 2-8 times a year to keep the T inventory under the 640g limit. Efficiency on co-deposited mix-layers (e.g; Be-W layers) and/or on co-deposits formed at temperature close to that of baking requires however further investigation. Experiments on the JET-ILW, with a baking capability up to 320°C, should confirm the ability of the technique for this purpose.

High fluxes evidenced in ICWC discharge make this technique particularly attractive. The ion flux parallel to magnetic field lines (10^{21}ions.m^{-2}) is expected to be more homogeneous on the ITER conformal First Wall than in current experiments, where interaction is mainly on limiters,

Bohm diffusion governing the radial decay of ions in the edge of ICWC plasmas. Since the first quantification of high fuel removal by isotopic exchange by ICWC plasmas on TORE SUPRA [4], a database on fuel removal efficiencies has been constituted with data from TORE SUPRA, TEXTOR, ASDEX-Upgrade, JET-CFC and JET-ILW [31]. Table 2 summarizes the measured efficiencies for H_2 (or D_2) ICWC for fuel removal by isotopic exchange. Amounts removed are given in monolayers of D (resp. H) atoms (one monolayer corresponds to a surface coverage of 2.10^{19} atoms.m^{-2}). Values given in Table 2 were obtained from shot-based measurement of partial pressures, integrated over RF pulse and several characteristic pumping times.

With about 30 minutes available for inter-pulse ICWC [31], T-removal efficiency in ITER can be extrapolated considering the given ICWC discharge durations and subsequent pumping times in each machine [31]. Given the characteristic pumping time in ITER (≈ 40s), about ten 3s long ICWC discharges, each followed by 120s post-discharge could be performed and remove up to 0.4gT between plasma shots, i.e. an amount comparable to that of the estimated retention per pulse [11, 12], ICWC is therefore considered as an efficient option to mitigate the T inventory buid-up, as in the so-called "good housekeeping approach" [43].

Although recovery from disruption has been successfully demonstrated on JT60-U [5] with ECWC only, little data exist on fuel removal. The few results reported in the literature indicate a lower efficiency than ICWC. Considering the low absorption of ECRH power in these low temperature discharges and the associated risk to damage in-vessel PFCs or diagnostics, the application of the ITER ECRH system for wall conditioning is also still pending assessment. It should be however stressed that operational conditions (input gas pressure, ECRH power) should be very similar to those encountered in ECRH-assisted plasma start-up in ITER, which is a functional requirement of the ECRH system [25]. More effort is anyway required to quantify efficiency on current devices.

Despite removed quantities comparable to that of ICWC or L-mode plasma in the JET- ILW, GDC operation requires the absence of toroidal magnetic field, and it can therefore not be used in the silent time between ITER plasma pulses to control T inventory in ITER. In this respect GDC is not expected to be an attractive tool for T-removal.

ACKNOWLEDGEMENTS

This work was supported by EURATOM and carried out within the framework of the European Fusion Development Agreement. The views and opinions expressed herein do not necessarily reflect those of the European Commission.

ITER DISCLAIMER

The views and opinions expressed herein do not necessarily reflect those of the ITER Organization.

REFERENCES

[1]. J. Winter, Plasma Physics and Controlled Fusion **38** (1996) 1503–1542

[2]. J. Roth et al., Plasma Physics and Controlled Fusion **50** (2008) 103001

[3]. A. Lyssoivan et al., Nuclear Fusion **32**, 1361 (1992)

[4]. D. Douai et al., Journal of Nuclear Materials **415** (2011) S1021– S1028

[5]. K. Itami et al., Journal of Nuclear Materials **390–391** (2009) 983–987

[6]. D. Douai et al. Journal of Nuclear Materials **438** (2013) S1172–S1176

[7]. G. F. Matthews et al Journal of Nuclear Materials **438** (2013) S2–S10

[8]. E. Joffrin et al, Nuclear Fusion **54** (2014) 013011 (12pp)

[9]. N. Fedorczak et al., this conference

[10]. S. Brezinsek et al, Journal of Nuclear Materials **438** (2013) S303–S308

[11]. S. Brezinsek et al, Nuclear Fusion **53** (2013) 083023 (13pp)

[12]. M. Shimada, R.A. Pitts, Journal of Nuclear Materials **415** (2011) S1013–S1016.

[13]. M. Baldwin et al., Journal of Nuclear Materials **438** (2013) S967–S970

[14]. M. Baldwin et al., Nuclear Fusion **54** (2014) 073005 (9pp)

[15]. K. Sugiyama et al., Journal of Nuclear Materials **415** (2011) S731–S734

[16]. K. Sugiyama et al., Journal of Nuclear Materials **438** (2013) S1113–S1116

[17]. S. Murayama, Proceedings of the 24th IAEA FEC, San Diego, USA (2012), Paper ITR/P5-24

[18]. G.J.H Hagelaar et al., submitted to Plasma Physics and Controlled Fusion.

[19]. D. Kogut et al., submitted to Plasma Physics and Controlled Fusion.

[20]. P. Andrew et al., Fusion Technology **94**, p. 203

[21]. D. Kogut et al., this conference.

[22]. G. Saibene et al., Journal of Nuclear Materials **220–222** (1995) 617–622

[23]. V. Philipps et al., 22nd IAEA Fusion Energy Conference (Geneva, Switzerland, 2008), Paper FT/4-2Ra

[24]. A0 GDRD 3 01-07-19 R1.0, Design Requirements and Guidelines Level 2 (DRG2), ITER (2006)

[25]. ITER Project_Requirements_(PR)_27ZRW8_v4_6, (2010)

[26]. J. Snipes et al. 7th IAEA Technical Meeting on Steady State Operation of Magnetic Fusion Devices (Aix en Provence 2013)

[27]. T. Wauters et al., Journal of Nuclear Materials **415** (2011) S1021–S1028

[28]. T. Wauters et al., Plasma Physics and Controlled Fusion **53** (2011) 125003 (20pp)

[29]. Dong Su LEE, Suk-Ho Hong et al., Trans. Fusion Science and Technology, **60**, 2011 94-97

[30]. A. Lyssoivan et al., Plasma Physics and Controlled Fusion **54** (2012) 074014 (25pp)

[31]. D. Douai et al., Proceedings of the 24th IAEA FEC, San Diego, USA (2012), Paper EX/P5-09

[32]. E. Gauthier, Journal of Nuclear Materials, Volumes **241–243**, 11 February 1997, Pages 553–558

[33]. T. Wauters, 2011 PhD Thesis Gent University Belgium, ISBN 978-90-8578-458-6

[34]. J. li et al., Journal of Nuclear Materials **415** (2011) S35–S41

[35]. E. Gauthier et al., Proc. of the 28th EPS Conference, 2001, paper P5.094

[36]. K. Itami et al., Journal of Nuclear Materials **438** (2013) S930–S935
[37]. J. Stober et al., Nuclear Fusion **51** (2011) 083031 (9pp)
[38]. D. Douai, et al, Proc. of the 40th EPS Conference, 2013, paper **P2**.120
[39]. A. Lyssoivan et al., 20th Topical Conference on RF Power in Plasmas (Sorrento, Italy 2013) AIP/CP-1580 , **287–290**
[40]. T. Wauters et al., this conference
[41]. T. Loarer et al., this conference
[42]. T. Wauters et al., 20th Topical Conference on RF Power in Plasmas (Sorrento, Italy 2013) AIP/CP-1580, **187–190**
[43]. G. Counsell et al., Plasma Physics and Controlled Fusion **48** (2006) B189–B199

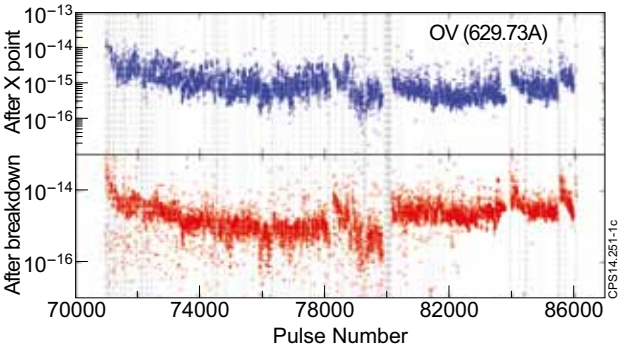

Figure 1: Normalized OV line intensity in plasmas either following breakdown (bottom) or after X-point formation (top). Units are 10^6 counts/m^2/s GDCs are represented by dashed grey lines.

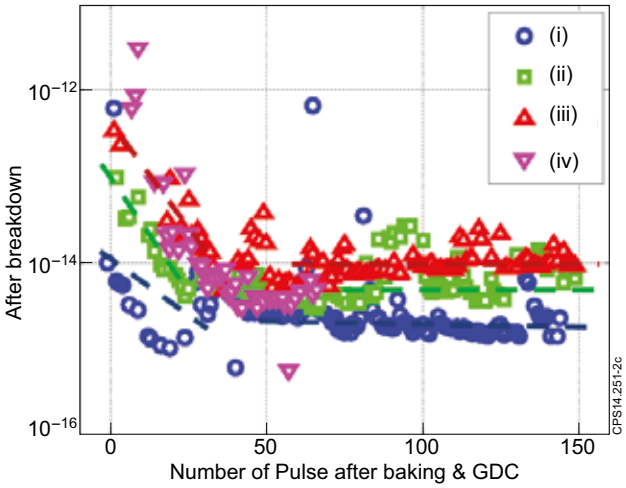

Figure 2: Normalized OV line intensity in the first 3 s after breakdown of JET-ILW plasmas following right at restart after the different conditioning cycles (see text). Units are 10_6 counts/m^2/s.

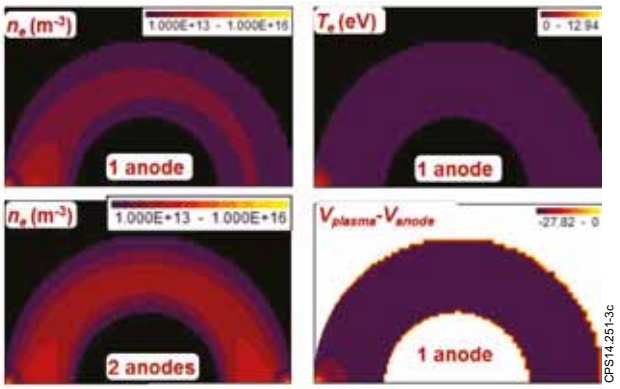

Figure 3: Spatial distribution of plasma density, temperature and potential in a simulated H_2-GDC in ITER at 0.3Pa and 30A. The anode potential for these conditions is 375V.

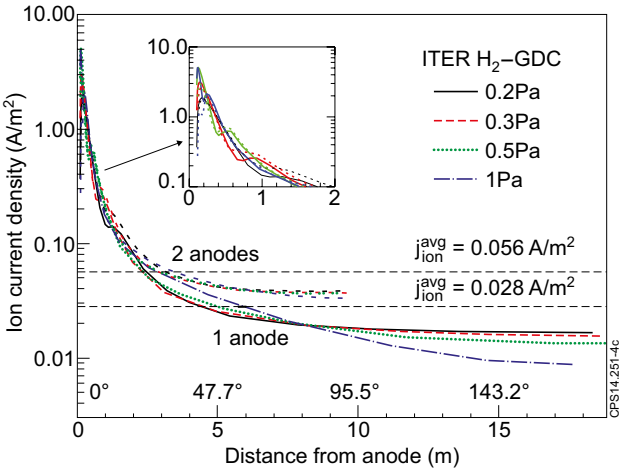

Figure 4: Ion current density distribution over outer wall as a function of the toroidal distance along the wall simulated for ITER H_2-GDC at 0.3Pa and 30A. The inset shows zoom-in close to the anode.

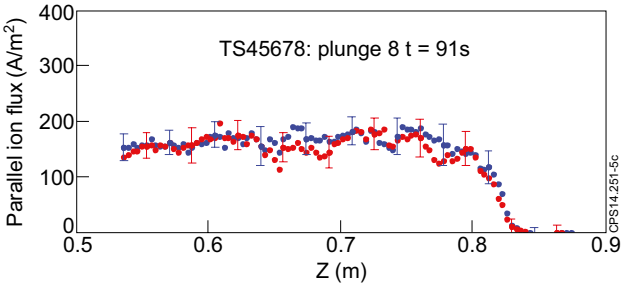

Figure 5: Ion current measured by a retarding field analyser in a TORE SUPRA He-ICWC discharge (B_T = 3.8T, f = 48MHz, $P_{RF,gen}$ = 300kW, $p_{He} = 2 \cdot 10^{-2}$Pa) at the ion (red) and electrons (blue) side collectors.

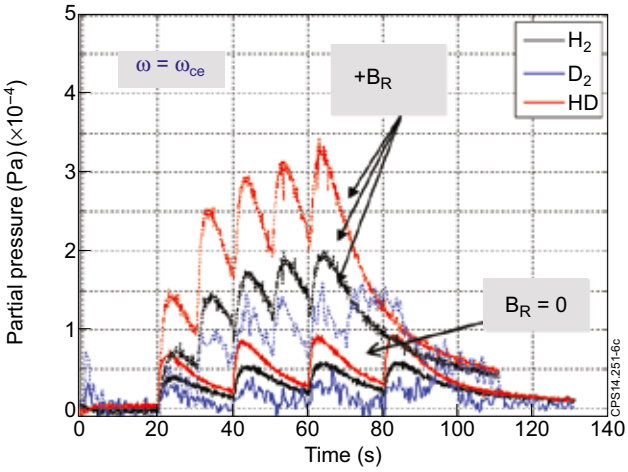

Figure 6: H_2, D_2 et HD partial pressures in two He-ECWC discharges (B_T = 3,8T, f = 110GHz, $p_{He} = 5.10^{-2}$Pa), without (full lines) and with (dashed lines) application of a small radial field.

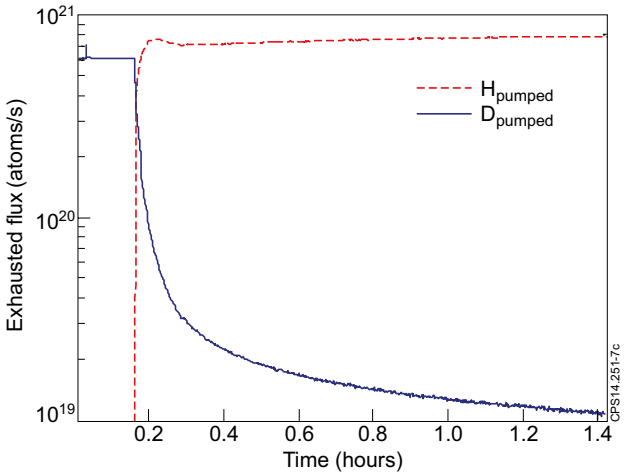

Figure 7: Temporal evolution of the exhausted hydrogen (red) and deuterium (blue) fluxes during change-over from D_2 to H_2-GDC ($p = 3.10^{-3}$ mbar, U = 500 Volts)

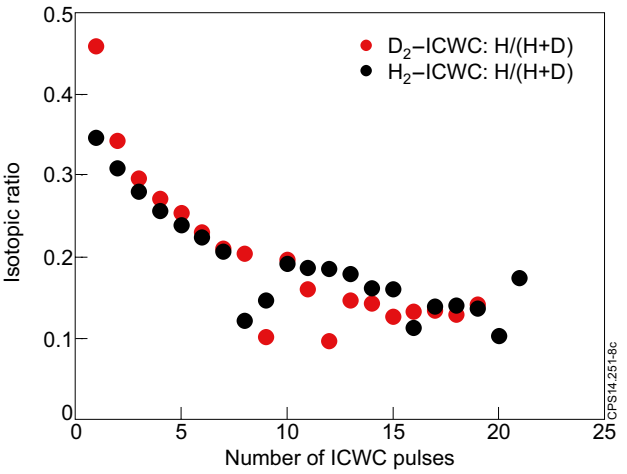

Figure 8: Evolution of the isotopic ratio in a D_2-ICWC on JET-ILW, preloaded with H_2-GDC (red dots) and in a H_2-ICWC on JET-ILW without preloading.